Electrical Power and Energy Systems 148 (2023) 108923

Contents lists available at ScienceDirect

International Journal of Electrical Power and Energy Systems

journal homepage: www.elsevier.com/locate/ijepes

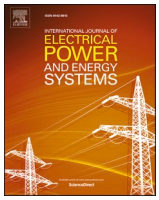

# Master-slave strategy based in artificial intelligence for the fault section estimation in active distribution networks and microgrids

J. Atencia-De la Ossa [a], C. Orozco-Henao [a,*], J. Marín-Quintero [b]

[a] Department of Electrical and Electronic Engineering, Universidad del Norte, Barranquilla, Colombia
[b] Electric and Electronic Engineering Program, Universidad Tecnológica de Bolívar, Cartagena, Colombia

ARTICLE INFO

*Keywords:*
Fault section
Active distribution networks
Microgrids
Artificial Intelligence

ABSTRACT

Fault location plays an essential role in the integration of self-healing functionalities in active distribution networks and microgrids. However, the fault location methods formulation presents great challenges for these types of networks because the operating changes that occur them, such as changes in topology, DER connection/disconnection and microgrids operating modes. Several fault location solutions have been proposed; nevertheless, these are strongly dependent on robust communication systems. This paper presents an artificial intelligence-based master–slave strategy for the estimation of the fault section in active distribution networks and microgrids using dispersed measurements. The strategy is composed by two stages. The master stage uses a genetic algorithm that determines the location and number of devices which maximize the faulted location e performance. The slave stage uses artificial neural networks to predict the fault section by using local voltage and current measurements trough an intelligent electronic device (IED). This approach is useful because it neglects the need of a robust communication systems and synchronization process between measurements. Here, each IED estimates the faulted section and then sends it through the single communication system to the distribution system operator control center. The presented method is validated on the modified IEEE 34-nodes test feeder where the accuracy of the strategy was 95%. The results obtained and its easy implementation indicate potential for real-life applications.

## 1. Introduction

The transition from conventional power distribution networks to active distribution networks (ADN) and the implementation of Microgrids (MG) have increased the reliability, energy efficiency and resilience of electrical distribution systems [1]. To improve the resilience and reliability, these networks lean on the development of fault location methods. However, the penetration of Distributed Energy Resources (DER) and MGs introduce new aspects that the conventional fault location (FL) approaches do not consider [2]. Several approaches have considered in a partial way the DER integration and MGs [3]. On the other hand, some impedance-based FL methods have formulated the effect of DERs. In [4] an approximate synchronous machine model is used to estimate the contribution of DERs to the fault. However, inverter-interfaced DER (IIDER) are not considered. Additionally, in [5] the effect of the DER is considered by using an IIDER analytical model. However, it does not take in account the effect of inverter-non interfaced DER (INIDER). In [6–8], a FL method that uses both synchronized measurements and a DER model are presented. Nevertheless, operational conditions as MG operation modes and the FL formulation does not contemplate. [9–12] use a traveling wave- based approach for fault location. Traditionally, this approach has been proposed for transmission lines. However, [13] demonstrates that this method is accurate for distribution systems like impedance-based methods. In [10] is presented a fault location method for radial distribution network by using reclosure-generating traveling waves. This method can only be used for the location of permanent faults, and it is not suitable for feeders which do not allow reclosing operation. Additionally, DER integration and MGs are not contemplated. [9] proposes a fault classification method by using discrete wavelet transforms for distribution systems with wind power distributed generation. This method classifies the fault type, but it does not locate them. Additionally, the operating conditions of ADN, such as topology changes, intermittency of DERs, and MG operation modes are not considered in its formulation. Still, there are some challenges to deal in fault location problem such as the estimation of multiple fault distances, the presence of MG into the ADN and the equipment requirements for a high sampling rate.

On the other hand, the fault location approaches have regarded the

* Corresponding author.

https://doi.org/10.1016/j.ijepes.2022.108923
Received 3 June 2022; Received in revised form 13 October 2022; Accepted 21 December 2022
Available online 2 January 2023

use of machine learning techniques, such as Support Vector Machine (SVM), Artificial Neural Networks (ANN), Fuzzy Logic System (FLS) in the last years. Some of these approaches use wavelet transform for transients processing and improving FL method performance. In [14–16], ANN-based fault location strategy is proposed. This approach is formulated into two stages. The first stage trains an ANN model to determine the fault type, and the second stage determines the section in fault. The test considers load variation, and integration of DG; and [14] considers topology changes and high-impedance fault. However, DER connection/disconnection, different technologies of DER and MG operation modes are not considered.

FL methods with integration of ADN and MGs have also been proposed in [8,17]. Still, they do not consider the operational conditions as off/on grid modes of MGs and DER connection/disconnection. Finally, FL methods have been formulated considering wide-area synchronized current and voltage phasors measurements provided by digital fault recorders and Global Positioning System (GPS) [14–16,18–20]. These methods are robust, however depend strongly on the availability of the sparse measurements and their synchronization. Other works use wide-area non-synchronized measurement, although they are still dependent on the presence of a significant number of meters installed in the ADN. Furthermore, these methods do not determine the number and location of measurement devices necessary to achieve adequate performance of the fault location technique [21].

The previous information can be summarized in Table 1 which presents the main works of state-of-the-art, and the aspects faced by them. Also, it highlights some challenges to face in the FL formulation for ADN and MG.

The main challenges are associated with considering the main ADN operating conditions, reducing the dependence of the LF formulation on the availability of the communication system, and considering the high-impedance faults and low-impedance faults.

This work addresses the first two challenges by a master–slave strategy based in artificial intelligence for the estimation of the fault section in ADN and MG using dispersed measurements. The approach considers that ADN has an integrated Advanced Distribution Automation (ADA) system and all its IEDs can be used as fault section estimators. Thus, in this strategy, the master stage uses a genetic algorithm to determine the location and number of IEDs that maximize the faulted section estimation performance. The slave stage uses ANN to introduce the ability to each IED to determine the fault section using local voltage and current measurements. This eliminates the need for robust communication systems and synchronization process between measurements, since each IED estimates the faulted section and sends it through the single communication system to the distribution system operator control center. The faulted section is determined from the faulted sections located by each IED. The main contributions of this work towards the state-of-the-art are:

- Considering the main ADN operating conditions in FL formulation, such as topology changes, DER connection/disconnection, and microgrid operation modes (on-grid and off-grid).
- Reducing of FL strategy dependency on robust communication system availability and synchronization processes between measurements for precise location of the fault.
- Determining of number and location of the IED that allows maximizing the faulted section estimation performance.

The remaining of this paper is organized as follows. Section 2 presents the formulation of an ANN model as fault section estimator and its integration into an IED. Section 3 explains the artificial intelligence-based master–slave scheme for the estimation of the fault section. Section 4 illustrates the cases of studies, and Section 5 presents the relevant implementation aspects of FL strategy. Section 6 shows the results and discussion, and the main conclusions of this work are presented in Section 7.

## 2. Formulation of an ANN model as fault section estimator to be integrated in an IED

Consider the ADN presented in Fig. 1. The system can change its topology through the switchgears $sw_1$, $sw_2$ y $sw_{MG}$. Also, it contains a MG which can connect and disconnect through $sw_1 and sw_{MG}$.

Additionally, we can include a fault in the node 812. Then, the

**Table 1**
Comparison of the state of the art for fault location methods.

| Aspect | References | | | | | | | | | | | | | | | | | | |
|---|---|---|---|---|---|---|---|---|---|---|---|---|---|---|---|---|---|---|---|
| | [4] | [5] | [6] | [7] | [8] | [9] | [10] | [11] | [12] | [13] | [14] | [15] | [16] | [17] | [18] | [19] | [20] | [21] | PM |
| *IED and communication architecture* | | | | | | | | | | | | | | | | | | | |
| Determine the number and location of IED | x | x | x | x | x | x | x | x | x | x | x | x | x | x | x | x | x | x | √ |
| Consider sparse measurements | x | x | x | x | √ | x | x | √ | √ | x | √ | √ | √ | √ | √ | x | √ | √ | √ |
| Can use synchronized measurements | x | x | √ | x | √ | x | x | √ | √ | x | √ | √ | √ | x | √ | x | √ | √ | √ |
| Can use unsynchronized measurements | √ | √ | x | √ | √ | √ | √ | x | x | x | x | x | x | √ | x | x | √ | x | √ |
| *ADN features considered* | | | | | | | | | | | | | | | | | | | |
| Unbalance | √ | √ | √ | √ | √ | √ | √ | √ | √ | √ | √ | √ | √ | √ | √ | √ | √ | √ | √ |
| Topology changes | x | x | x | x | x | x | √ | x | x | x | √ | x | √ | x | x | x | x | x | √ |
| Load change | x | x | x | x | x | x | √ | x | x | x | √ | x | x | √ | x | x | x | x | √ |
| DER technologies (IIDER and INIDER) | x | x | x | √ | √ | x | x | x | x | x | x | x | x | x | x | x | x | x | √ |
| Several DER connected | √ | √ | x | x | √ | x | x | √ | √ | √ | √ | √ | x | √ | x | √ | √ | x | √ |
| DER connection/ disconnection | x | x | x | x | x | x | x | x | x | x | x | x | x | x | x | x | x | x | √ |
| MG operation modes (on-grid/off-grid) | x | x | x | x | x | x | x | x | x | x | x | x | x | √ | x | x | x | x | √ |
| *Fault considerations* | | | | | | | | | | | | | | | | | | | |
| Fault types | √ | √ | √ | √ | √ | √ | √ | √ | √ | √ | √ | √ | √ | √ | √ | √ | √ | √ | √ |
| Low impedance faults | √ | √ | √ | √ | √ | √ | √ | √ | √ | √ | x | √ | √ | √ | √ | x | √ | √ | √ |
| High impedance faults | x | x | x | x | x | x | x | x | x | x | √ | x | x | x | x | √ | x | x | x |
| Deal with the multiple estimation problem. | x | x | x | x | x | x | x | x | √ | √ | √ | √ | √ | √ | x | √ | √ | √ | √ |

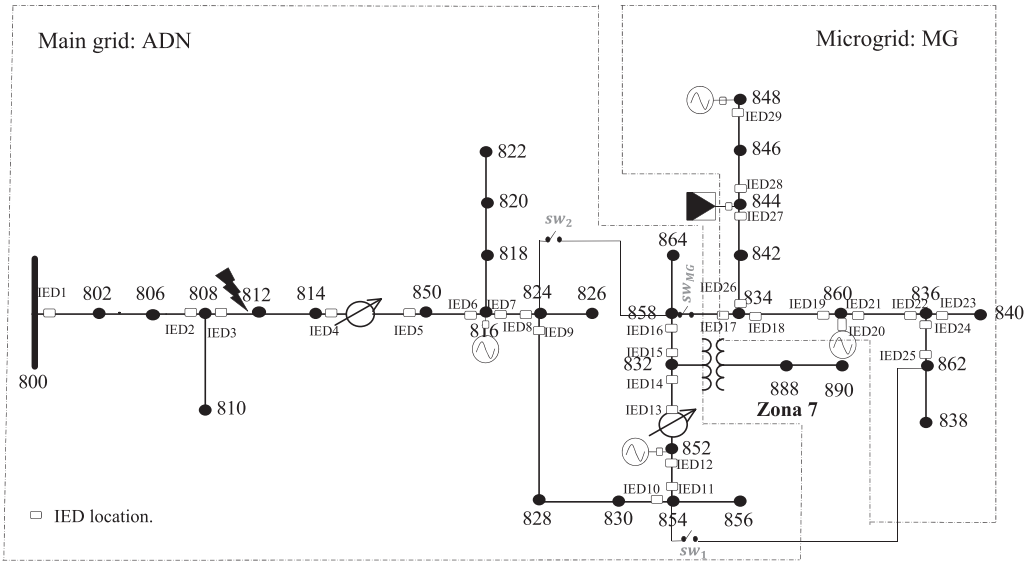


**Fig. 1.** ADN with a MG integrated.

protection system operates, and the ADA system begins the isolation of the fault and the restoration of the electricity supply. To improve the effectiveness of this process, a fault section estimator based on ANN model is integrated into each IED as shown in Fig. 2.

The faults section estimation problem can be formulated as a classifier to then obtain an ANN model. For this, the methodology divides the ADN and MG in sections as shown in Fig. 3, where we can see two possibilities. The first in Fig. 3(a), when we have IEDs in the main grid, here, the methodology defines a section to classify the faults that occur into MG (Section 8). The second in Fig. 3(b), when we have IEDs into MG, here, the methodology defines a section to classify the faults that occur in the main grid (Section 4).

The sections presented in Figs. 3 and 4 represents the classes of the ANN model, and the location of the fault associate with it. To obtain the ANN model a set of fault operating conditions must be considered, here each operating conditions have a fault location from a set of $n$ classes. Each operating condition presents a set of k features for the *i-th* IED as $\boldsymbol{x}_i = \{x_{1i}, x_{2i}, x_{3i}, \cdots x_{ki}\}$. The features are estimated from the local current and voltage signals. Therefore, the ANN model is composed by a dataset with a k feature and $n$ classes is presented in (1).

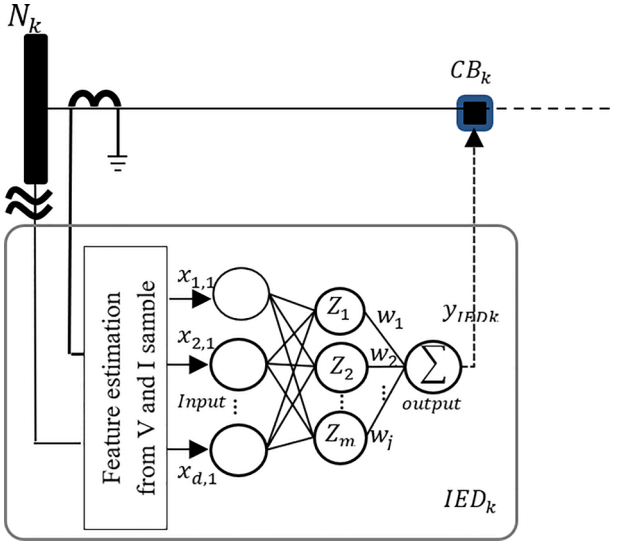


**Fig. 2.** Integration between the ANN model and IED.

$$y_{q_{IEDi}}(x_i, w) = \sigma\left(\sum_{j=1}^{m} w_{qj} \cdot \varphi(\gamma_j) + W_0\right)$$

s.a.

$$x_i \in R^d \quad i = \{0, 1, 2, \cdots, number\ of\ IEDs\}$$

$$\text{and } q = \{0, 1, 2, \cdots, n\}$$

Where, $\gamma_j = \sum_{m=1}^{k} \boldsymbol{w}_{jm} \cdot \boldsymbol{x}_{mi}$, $\boldsymbol{w}_{jm}$ and $\boldsymbol{w}_{qj}$ are the weight parameters, m is the number of neurons in the hidden layer, $\sigma$ and $\gamma$ are the active functions which the most common functions used are logistic sigmoid, hyperbolic tangent function and RBF [22].

In (1) we can observe that there is a class denominated 0, which is used to appoint the scenarios that do not present a fault condition, and instead they belong to a normal operating condition. Those scenarios must be analyzed because they can cause changes in the current and voltage signals measured by the IEDs. Additionally, the last class denominated $y_n$ gives to the DMS information about faults that take place out of its operating zone. This can be useful when a DMS and a MGCC work simultaneously in an active distribution network.

The complexity of the training of ANN model is proportional to the number of classes. Fig. 4 shows the generalized algorithm to obtain the ANN model for the IEDs installed into the ADN. The stages of the algorithm are explained in the following subsections.

### 2.1. Preliminary stage

This stage is composed by three steps. Each step is explained as below:

#### 2.1.1. Step I: Definition of the network information, IEDs locations, and sections

In this step, the methodology seeks to define the network information such as topologies, networks parameters, DER location, and normal and fault operating conditions. This information allows dividing the systems into different sections, as well, obtaining the dataset for training and validation.

The number of sections select to divide the systems must consider factors like the critical loads, zones of accessibility issues, and geographic area. In this research, we decide to define the sections according to the geographic area. Besides, each IED located along the system works beside with a digital relay belonging to the protection system.

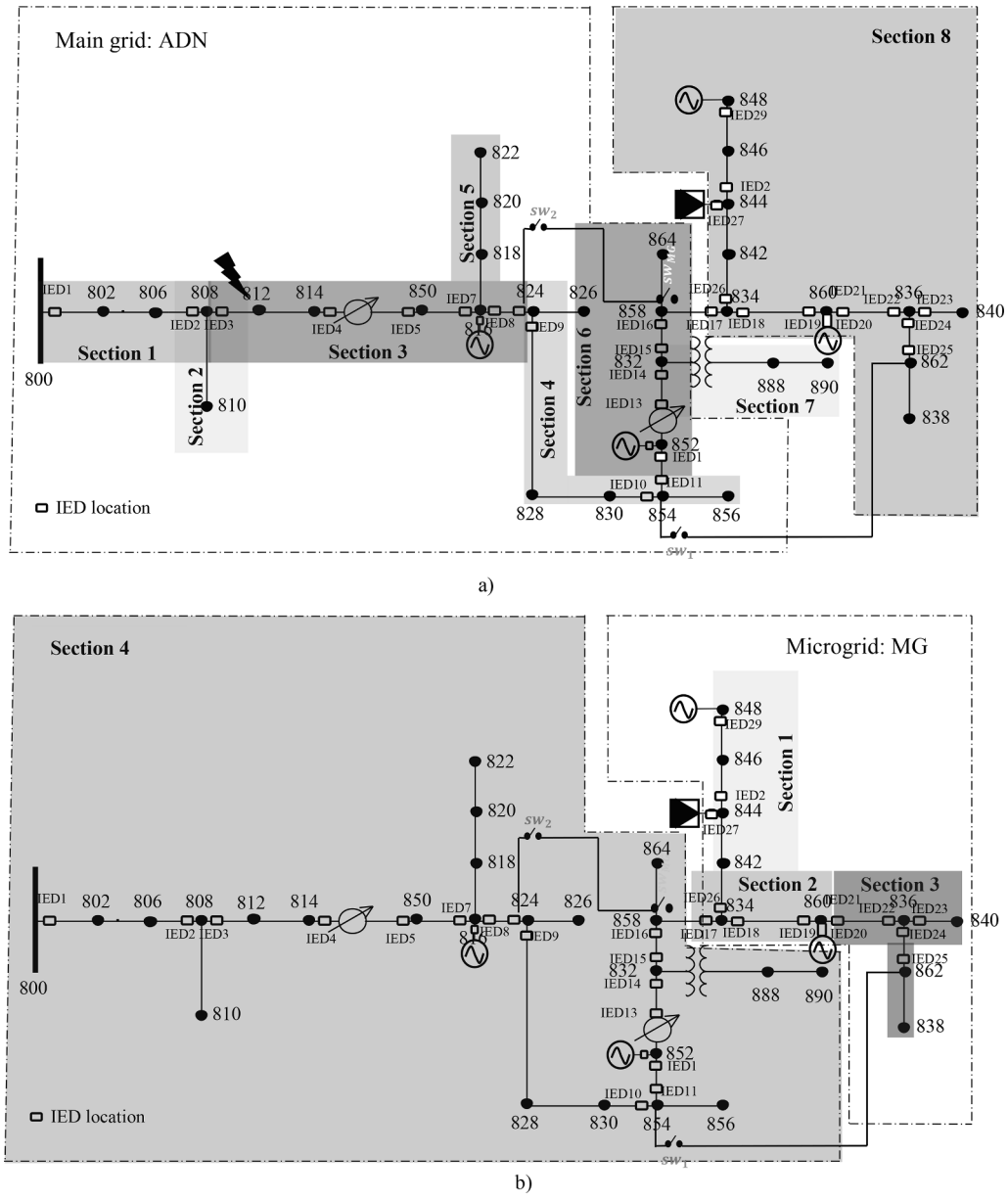


**Fig. 3.** Sections division proposed for the ADN.

*2.1.2. Step II: Database simulation*

The methodology has as a main premise that a high number of faults must be taken in account to obtain a reliable dataset and ANN model. However, the electric power systems are designed to reduce the probability of fault, that means that a dataset have to be composed by fault synthetic information. The synthetic dataset is obtained by a cooperative works between an EMT software and a numeric computing software as is presented in Fig. 5.

The proceeding to obtain the synthetic dataset is described as below.

- *ADN modeling and simulation:* The ADN can be modeled by using an EMT software. If the ADN involves a MG, as was presented in Fig. 1, the MG and main grid simulation must converge for each fault scenario simulated for when the MG operates in off-grid mode. [23].
- *Fault Scenario Generation:* The normal and fault operating conditions can be defined according to the stage 1. Once, the factors and levels are determinate. Table 2 presents the useful factors and levels for the formulation of the fault location and fault protection problems [24,25]. The number of operating conditions can be obtained with $= \prod_{k=1}^{n} \delta_k$, where $\delta_k$ is defined as the number of levels for the k-th factor.
- *Simulation of scenarios:* Before of simulating the normal and fault operating conditions we must run an optimal power flow (OPF) to determine the power injection of each DER. The OPF seeks to find a better point of operating, for this case, it minimizes the power losses. Then, the normal and fault operating conditions are simulated by EMT software. In this process, the strategy stores the current and voltage signals of each IED installed in the ADN.
- *Labeled of the fault scenarios:* the labeled process considers the section where was simulated each fault for the actual operating condition. If the network involves a MG as is shown in Fig. 1, the strategy independently labels both networks as shown in Fig. 3.

The result of this step is a dataset with the voltage and current signals in the location of the IEDS. Additionally, each fault operating conditions must be labelled according to its own section. The following steps explain how obtain the dataset.

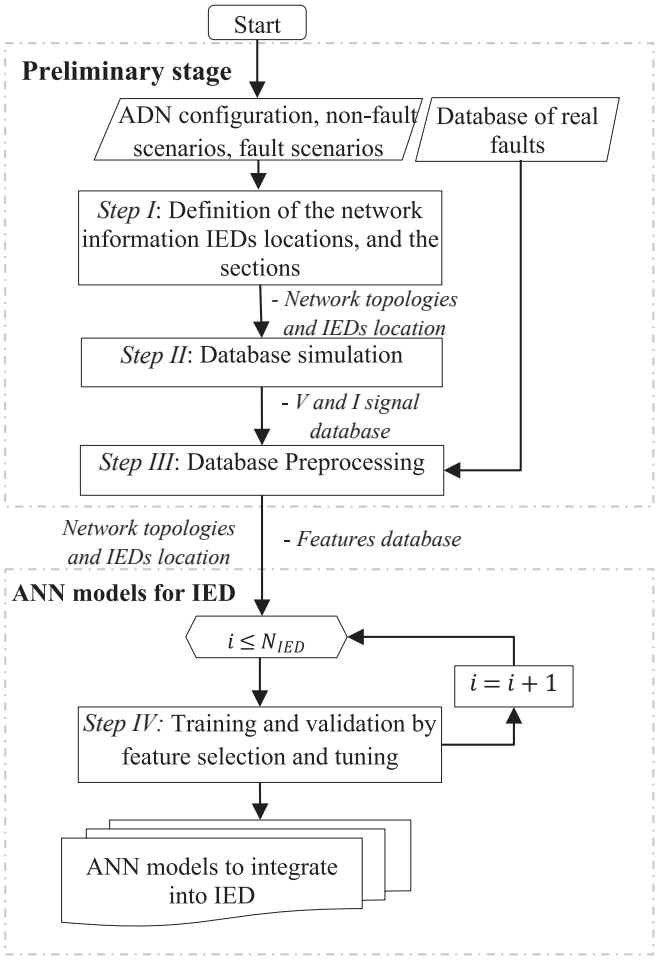


**Fig. 4.** Flow chart for the generation of the ANN model as a fault section estimator.

#### 2.1.3. Step III: Database processing

The dataset processing is made through three steps as below:

- *Feature Selection:* The features allow maximizing the performance of the ANN model used to identify a fault section. This process takes a relevant role for the ANN model construction because the performance can be affected by the increase or decrease of the dimensionality of the problem [26]. Several features have been proposed in the state of the art for the solution of the adaptive protection and fault location problem [242527]. In this research the features can be obtained by using a Fast Fourier Transform (FFT) where its phasor representation could be associated with the last cycle before of the fault (Pre-fault) and the last cycle registered (fault) as is showed in (2) and (3),

$$\cup^{p} = |\cup^{p}| \measuredangle \theta^{p}_{\cup} \tag{2}$$

$$\cup^{F} = |\cup^{F}| \measuredangle \theta^{F}_{\cup} \tag{3}$$

The features are defined as the difference between the fault and pre-fault values as are presented in (4) and (5).

$$d|\cup|_{w} = \cup^{F}_{w} - \cup^{p}_{w} \tag{4}$$

$$d\theta_{w} = \theta^{F}_{w} - \theta^{p}_{w} \tag{5}$$

Where $\cup$ is the magnitude of the current or voltage phasor for the phase $w$, and $\theta$ is the angle of the current or voltage phasor for the phase $w$. The superscripts F and p denote that the quantity will be obtained between the cycles of fault and pre-fault.

The combination of the features obtained by (2) and (5) allow generating new features such as the power, impedance, and power factor. Table 3 shows the most common features used in the state of the art by the fault location problems [242527].

- *Dataset standardization:* Once the dataset is obtained, it will be standardized by using (6). This process can improve the performance of the machine learning techniques as ANN or SVM [28].

$$x^{st}_{fm} = \frac{x_{fm} - \mu_{m}}{\sigma_{m}} \tag{6}$$

Where,

$x_{fm}$ is the value for the *f-th* fault operating scenario in the m-*th* feature,

$\mu_{m}$ is the average for the m-*th* feature,

$\sigma_{m}$ is the standard deviation for the m-*th* feature,

$x^{est}_{fm}$ is the standardized value for the f-*th* fault operating scenario in the m-*th* feature.

- *Dataset Splitting*: This research considers as rule of thumb split the dataset with rate equal to 4, where 80% of the dataset will be used to the training and 20% will be used to validate the ANN model [29].

### 2.2. ANN models for IED

#### 2.2.1. Step IV: Training and validation by using feature selection and tuning

In this step, the strategy obtains the fault section classifiers by training ANN models formulated in (1). Also, the strategy uses a Cuckoo Search Algorithm (CSA) to find the better combination of hyperparameters for ANN model with the main goal of improving its performance [30,31]. Also, the Algorithm 1 can select the best combination of features that maximize the accuracy indicator given in (7) for each ANN model in each IED.

$$acc_{i}[\%] = \frac{TNF_{i}}{TNS_{i}} \tag{7}$$

Where, *TNF* represents the number of fault operating conditions correctly located for the *i-th* IED and *TNS* is the total number of operating conditions considered for the *i-th* IED.

***Algorithm 1 - Cuckoo search algorithm***

***Input:*** *Database with the whole features*
***Output:*** *IEDs and its ANN model. Feature selection and tunning.*
***Begin***
*Set the initial value of the host nest size N, probability pa*$\in[0,1]$ *and maximum number of iterations* $M_G$.
*Set* $t = 1$. *{Counter initialization}*
***For*** $k = 1{:}N_{IED}$ ***do***
***For*** $j = 1{:}N$ ***do***
*Generate the j-th initial nest host* $x_j$. *The nest host are divided into two: attributes and hyperparameters.*
*Evaluate the fitness function for j-th initial nest: train and validate the k-th IED by the ANN technique with*
*setting defined by* $x_j$, *and obtain the performance of ANN model by (8)* $f(x_j)$.
***End For***
*Determinate the maximum value of* $f(x_j)$ *and save as* $f(x_j)^{max}$
***While*** $t \leq M_G$ ***repeat***
*Delete the worst nests and create new ones using the probability of worse nests to be abandoned (pa)*
*Update each nest by levy flights for hyper-parameters and levy flights and sigmoid function for the*
*attributes solution by (9) to (11).*
*Keep the best solutions (nests with quality solutions)*
*Rank the solutions and find the current best solution*
*Determinate the maximum value of* $f(x^{t}_{j})$ *and update if needed* $f(x^{t}_{j})^{max}$
*Set* $t = t + 1$. *{Iteration counter increasing}*
***End While***
*Produce the best solution for* $IED_k$: *ANN model, attributes and hyperparameters*
***End For***
***End***

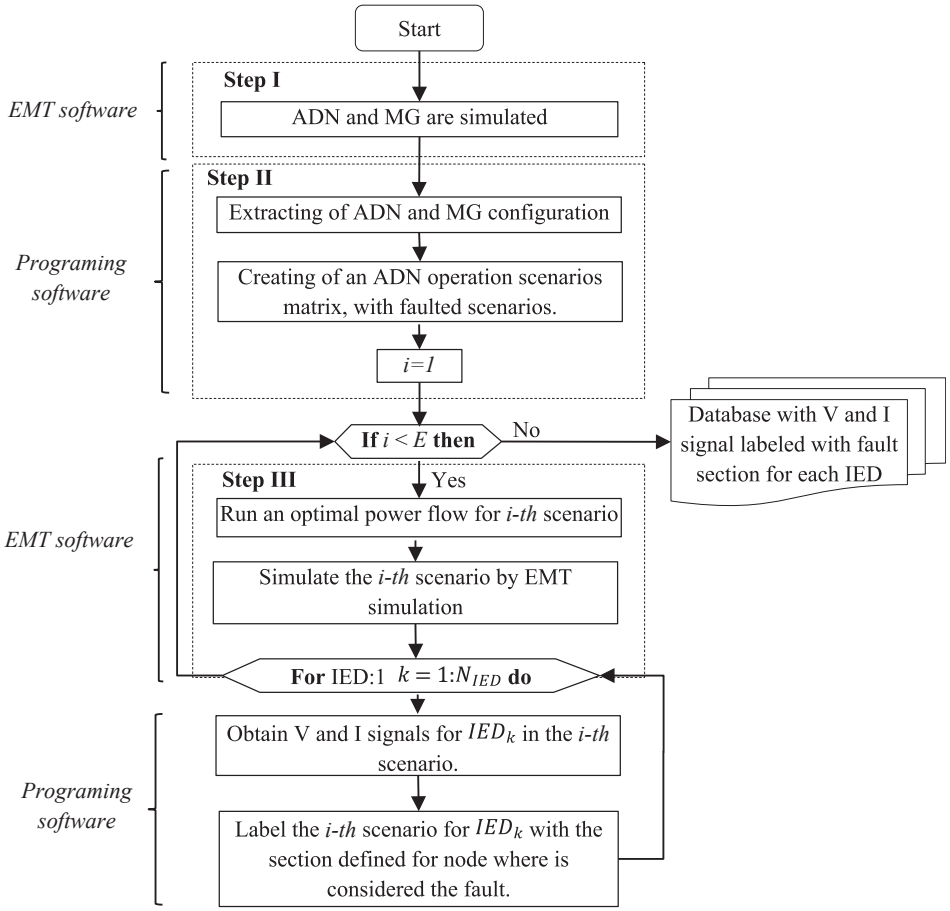


**Fig. 5.** Database simulation flowchart.

**Table 2**
Factors and levels commonly used in ADN operating scenarios.

| Group | Factor | Levels |
|---|---|---|
| No-fault operation | Load change | 30%-150% |
| | Generation change | 50%-150% |
| | Topology change | Reconfiguration, DER outage, and MG in off-grid mode |
| | Operation mode of microgrid | On-grid/off-grid |
| Fault operation | Fault type | Single-phase faults, double-phase faults, double-phase to ground faults and three-phase faults |
| | Fault location | Overall, ADN nodes |
| | Fault resistance | 0 Ω to 50 Ω |

**Table 3**
Features used in protection and fault location strategies.

| N° | Feature | Description |
|---|---|---|
| *1–3* | $dV_{abc}$ | Difference between voltage magnitude for instances of fault and pre-fault for each phase |
| *4–6* | $d\theta_{Vabc}$ | Difference between voltage angle for instances of fault and pre-fault for each phase |
| *7–9* | $dI_{abc}$ | Difference between current magnitude for instances of fault and pre-fault for each phase |
| *10–12* | $d\theta_{Iabc}$ | Difference between current angle for instances of fault and pre-fault for each phase |
| *13–15* | $dZ_{abc}$ | Difference between the impedance for instances of fault and pre-fault for each phase |
| *16–18* | $dS_{abc}$ | Difference between the apparent power for instances of fault and pre-fault for each phase |

The nests are updated through a levy flight function given in (8).

$$x_j^{t+1} = x_j^t + \propto \oplus Levy(\lambda) \tag{8}$$

When the nests have objects as the features, they can be updated according to the sigmoid function given in (9)-(10).

$$S(x_j^t) = \frac{1}{1+e^{-x_j^t}} \tag{9}$$

$$x_j^{t+1} = \left\{ \begin{array}{ll} 1 & if\ S\left(x_j^t\right) \rangle \sigma \\ 0 & otherwise \end{array} \right\} \tag{10}$$

The strategy implements the ANN models into the IEDs located along of the ADN, in this way, they are capable to estimate the fault section only with the local current and voltage measurements.

## 3. Artificial intelligence-based master–slave scheme for the estimation of the fault section.

The centralized communication architecture of the ADA system allows to each IED send the fault section estimated toward a control center. In this way, a unique fault section can be defined from the previous sections for each IED. For this process, the strategy uses the IEDs which have the duty of protecting the ADN system. However, the higher number of IEDs, the worse is the performance for the strategy, in this way, ANN models must be obtained for each IED. Additionally, as presented in [25], the individual performance of IEDs depends on their location in the network. Considering the above, this research presents a

master–slave strategy based on artificial intelligence to determine the number and location of IEDs which maximize the performance of a centralized fault section locator. The master–slave strategy is presented in Fig. 6.

The stages that compose the strategy will be described in the sections below.

### 3.1. Preliminary stage

In this stage, we can obtain the fault dataset used to train the ANN models which would estimate the fault section. The strategy uses the information given in the Section 2.1 to accomplish this task.

### 3.2. Master-slave stage

The master–slave strategy uses AI to find the number of IEDs and their location that maximize the performance of a centralized fault section locator who is into the control center. This strategy has as master stage a genetic algorithm which determine the optimal location of IEDs. The slave stage proposes an ANN model per each IED to estimate the section of the fault. Fig. 7 presents the flow chart for the genetic algorithm that works into the master–slave strategy to find the optimal location of IEDs. Subsections 3.2.1 to 3.2.4 presents the description of the algorithm steps.

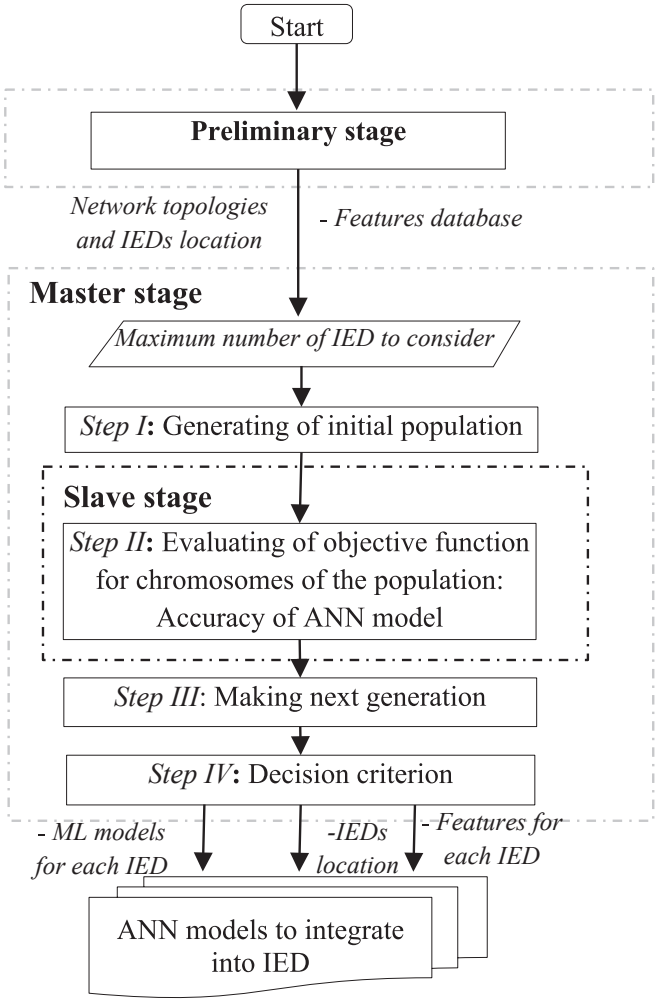


**Fig. 6.** Flow chart for the master -slave strategy based in artificial intelligence for the fault section estimation in ADN and MG.

#### 3.2.1. Step I: Initial population

The initial population can be divided in two segments. The first represents the population for the location of the IEDs into the main grid denominated $h_n^{(1)}$, and the second represents the population for the location of the IEDs into the MG named $h_n^{(2)}$. Both populations could be obtained in a random way through a uniform distribution. Also, it must consider the maximum number of IEDs (N) for each subsystem (main grid and MG). To formulate the chromosomes, a binary codification can be used, here N genes compose each chromosome. Each gene represents the location of one IED into the ADN used to estimate the fault section. The value of each gene can be zero (0) or one (1), where one (1) indicates that the IED will have an ANN model to estimate the fault section, and zero (0) indicates that the IED will not select. Each chromosome has a performance indicator which will be defined in the next stage.

#### 3.2.2. Slave stage implementation

Consider a set of fault scenarios denominated as P, which has a fault section for each scenario that can be estimated by using the information of each chromosome that composes the initial population $h_n^{(1)}$ and $h_n^{(2)}$. Each gen of chromosome locates the fault section $y_{IED_i}$, with an accuracy for its ANN model $acc_{IED_i}$ as is presented in Fig. 8.

To assess the fitness function for each chromosome for P, the IEDs that compose the *i-th* chromosome estimate the fault sections and report them to the control center (DMS or MGCC). Then, a unique fault section can be obtained by processing the fault sections gave by all IED as in Fig. 9. From (1) note that a label could be defined to represent events that are not faults for IEDs. Also, the last label, $y_m$ for the IEDs in the main grid and $y_n$ for the IEDs into the microgrid, are to locate the faults that occur outside the coverage of the control center. For instance, the location of faults into the microgrid by IEDs installed in the main network and vice versa.

The DMS and MGCC estimate the fault section by using a statistic indicator as the mode. Then, the DMS and MGCC must determinate the final decision, which can be represented by two possibilities. The first represents that the DMS and MGCC do not find a fault into the network, in this case, the label must be 0. The second possibility poses that the network presents a fault, so a section $y_j$ is selected as the section in fault. However, an additional process must be executed to define if the fault is inside or outside of the main grid. The strategy propose that each central control must analyze the decision taken by their IEDs, where $y_{DMS}$ and $y_{MGCC}$ are the section of fault located by the DMS and MGCC, respectively. If the DMS does not observe a fault into the main grid, but the MGCC detect the section of fault, $y_{DMS} = 0 \,\&\, y_{MGCC} \neq 0$, what means that the final decision indicates that the fault is in the section $y_{MGCC}$ of the MG. A similar task must be executed when the MGCC does not observe a fault into the MG, but the DMS detect the section of fault, $y_{DMS} \neq 0 \,\&\, y_{MGCC} = 0$. The above indicates that each fault locator works in an independently way, however, both always must have a communication between the control centers.

The fitness function for each chromosome can be assessed with the accuracy obtained in (7) when the validation process is made.

#### 3.2.3. Stage 2: The offspring of the next generation

In this stage can be obtained the chromosomes that will be participated to consolidate the next generation by using the crossover operator. The strategy proposes three steps for accomplishing this process: selection, crossover, and mutation [32]. The first step uses a tournament selection to obtain the chromosomes that will participate in the crossover step. The tournament selection seeks to select several chromosomes, where the chromosomes with s higher performance could be a better likely to be chosen. The second step is the crossover. Here, we pick up two random number between 0 and the length of the chromosome (N), to then exchange the genes content between those values.

In this process we obtain two new chromosome or offspring, [32].

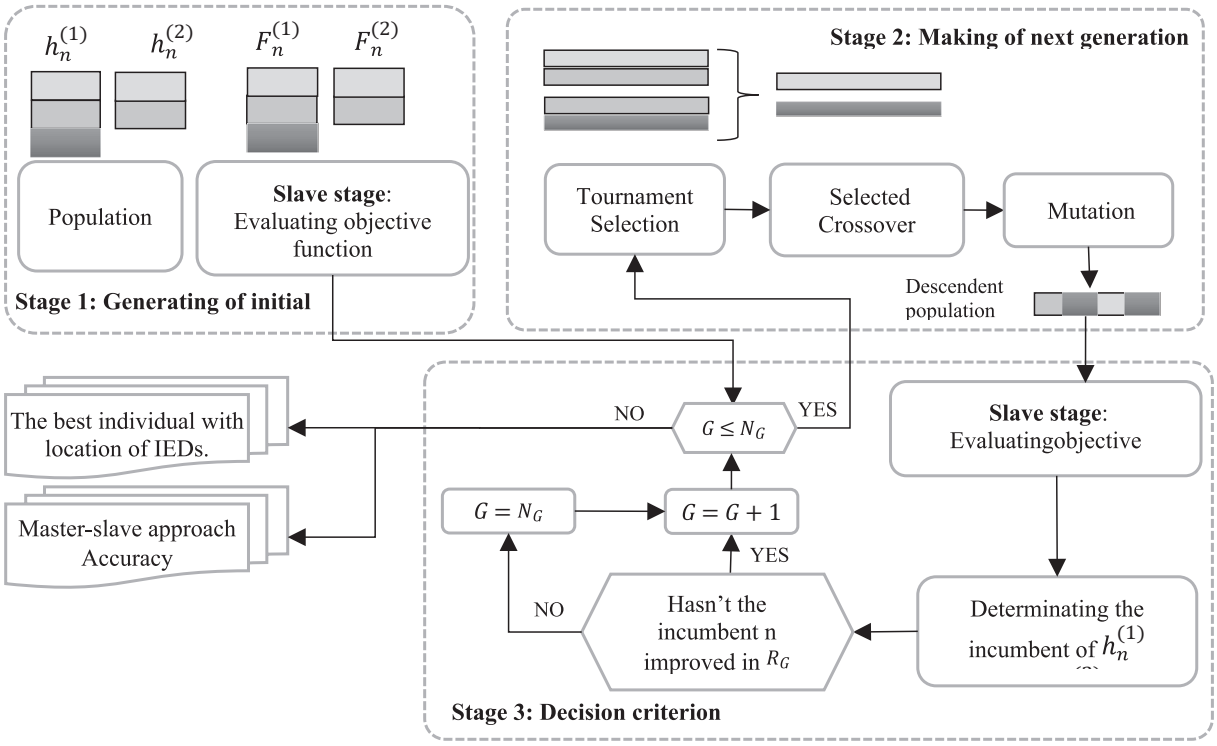


**Fig. 7.** Flowchart of optimal meter placement using Genetic Algorithm.

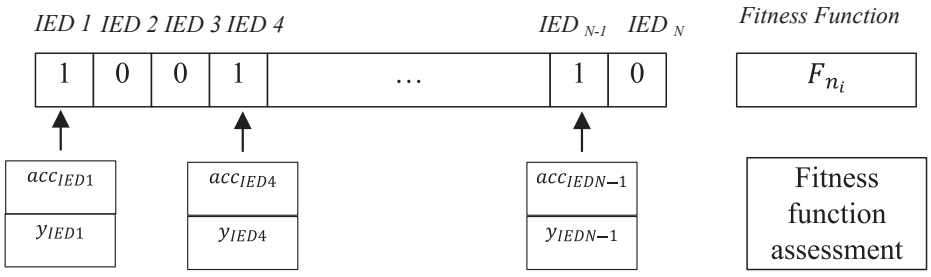


**Fig. 8.** Chromosome codification and fitness function assessment.

The last step is the mutation, here, a random gene of the chromosome can be modified according to a mutation rate $T_m$ which can be settled in values between 0.1 % and 5%. In this way, if this number is above of $(1 - T_m/100)$, the gene will become of 1 to 0 and vice versa. These three steps will be executed until obtain the offspring population.

### 3.2.4. *Step IV: Decision criterion*

In this stage can be calculated the fitness function for the offspring population by using the slave stage presents in the Section 3.2.2. Then, we can obtain the accuracy per chromosome, and determinate the incumbent solution for the offspring population $h_n^{(1)}$ and $h_n^{(2)}$ as the chromosome with the best performance. If the current incumbent solution is better than the previous, the global incumbent will be updated, and the process continues in the next generation. The genetic algorithm ends when the number of generations $N_G$ is reached or when the global incumbent solution has a number $R_G$ without being updated. The genetic algorithm gives as output the incumbent chromosome composes by the number and location of the IEDs that maximize the estimation of the section of the fault into the network. Additionally, the strategy allows obtaining the ANN models for each IED as is presented in Fig. 7.

## 4. Cases of studies

The proposed fault location strategy was validated by using the modified IEEE 34 bus test feeder shown in Fig. 1 [33]. This feeder has a voltage level of 24.9 k V. Some modifications were necessaries to become the test feeder in an active distribution network. The summary of the modifications are: adding four INIDER and one IIDER, inserting two switchgears to allow topological changes and integrating a MG capable to operate in islanded or grid mode. The method proposes as maximum number of IEDs 16, and 13, for the ADN and the MG, respectively. Table 4 presents the fault operating scenarios used to create the dataset. Also, the features used for the validation are consigned in Table 3 presented in the Section 2.1.3.

The proposed strategy was validated considering two cases as presented in the following sections.

### 4.1. *Case 1: ANN model as fault section estimator integrated into an IED*

In this case, we will train and validate the ANN models as a fault section estimator for each IED along of ADN and the MG by using the Cuckoo search-based tuning strategy. Table 5 presents the range of values considered for each hyperparameter in the tuning strategy. Also, we decide to use the features consigned in Table 3 to determine the best

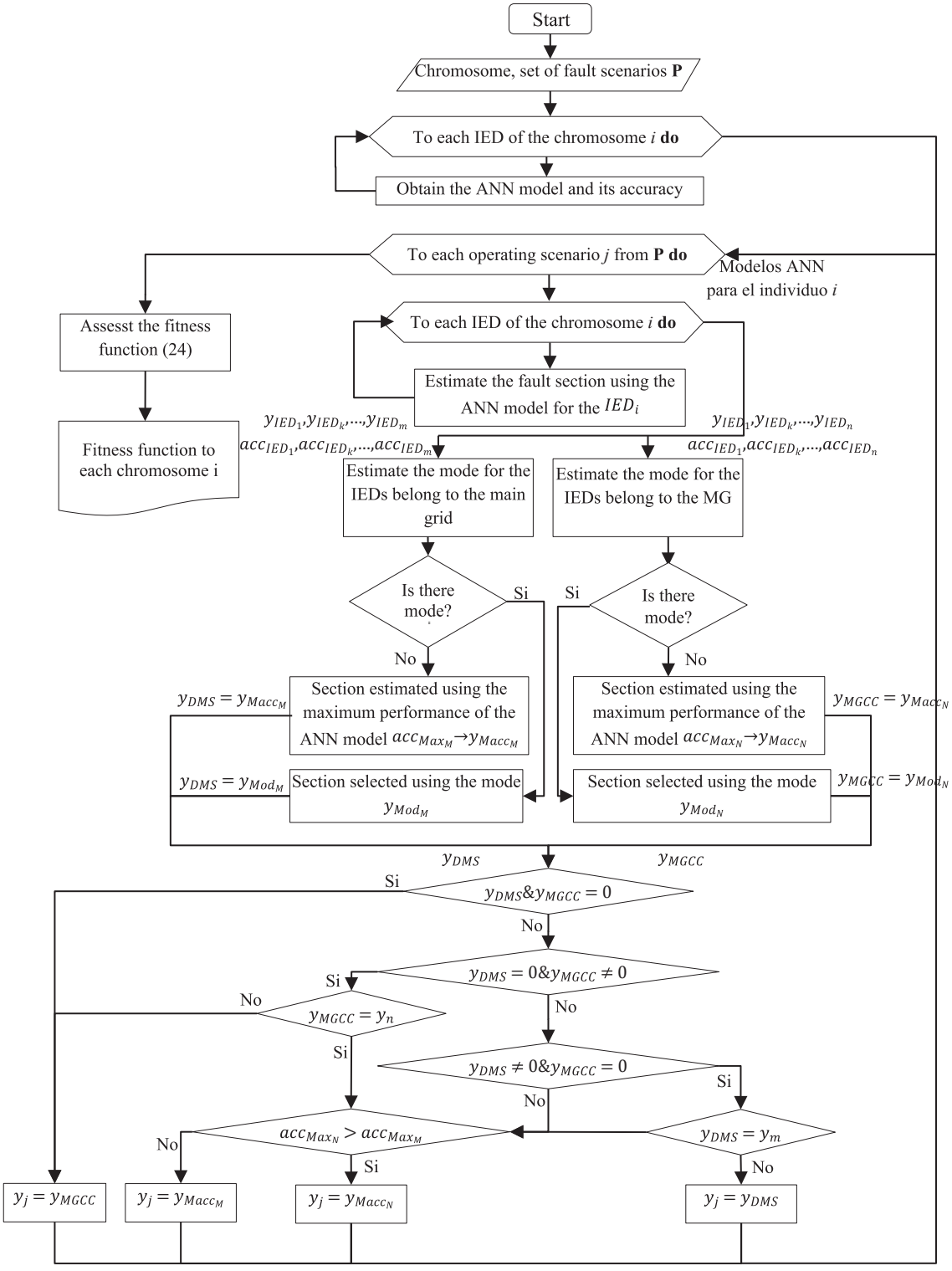


**Fig. 9.** Flow chart to assess the fitness function of each chromosome.

combination of them.

### *4.2. Case 2: Fault section estimator based in an artificial intelligence master -slave strategy*

In this case, we will seek to evaluate the performance of the strategy described in the Section 3. The master–slave strategy has as main goal find the number of IEDs and its location that maximize the performance of the centralized fault section estimator. Table 6 shows the genetic algorithm parameters used by the master–slave strategy.

## 5. Implementation of master–slave strategy for the fault section estimation

The master–slave strategy based in artificial intelligence for the fault section estimation was implemented using Power Factory DigSilent®

**Table 4**
Scenario proposed for method validation.

| Factors | Levels | Number of levels |
|---|---|---|
| Network topology | Top1: Original Network<br>Top2: Network with L824-L858 active.<br>Top3: Network with L854-L862 active.<br>Top4: Original network without the MG.<br>Top5: Network with L824-L858 active without the MG.<br>Top6: Original Network plus a load test feeder | 6 |
| Cut off generation | 0: Without cut off generation<br>3: Generator 3 out of service<br>4: Generator 4 out of service<br>5: Generator 5 out of service | 4 |
| Load change | 1: Low scenario (40% − 55%).3: Middle scenario<br>(71% − 85%).5: High scenario<br>(101% − 120%). | 3 |
| Fault resistance | 0, 20, 45 Ohms | 3 |
| Type of fault | Single phase to ground (A), Double phase fault (AB), three phase fault | 3 |
| Location of the fault | All the nodes | 36 |
| Total scenarios | $\#\mathscr{S} = \prod_{k=1}^{n} \delta_k$ Where $\delta_k$ is the number of levels of the factor $k$. | 23.328 |

**Table 5**
Hyperparameter tuning intervals.

| Hyperparameter | Levels |
|---|---|
| Number of Neurons | 0 – 200 |
| Hidden layers | 1–3 |
| Function of activation | Identity, logistic, tanh, relu |
| Solver | lbfgs, sgd, adam |
| Learning Rate | Constant, invscaling, adaptive |

**Table 6**
Genetic Algorithm Parameters.

| Parameters | Value |
|---|---|
| Number of chromosomes | 30 |
| Maximum number of generations | 500 |
| Limit of stabilization of the generations ($R_G$) | 40 |

and Python® as EMT software and programming language, respectively. The following subsections describe the most important considerations of the implementations of the cases studies.

### 5.1. Preliminary stage

We obtained the normal and fault operating scenarios according to the combination of the factors presented in Table 4. Additionally, the dataset was generated by 23.328 fault operating scenarios with a sampling rate of 128 samples/cycle, a simulation time of 200 ms, and the fault time of 100 ms. The current and voltage signals were obtained in the locations of the IED as shown in Fig. 1. On the other hand, we decide to divide the main grid in eight sections and the MG in four sections according to Fig. 2. Each fault operating scenario were labeled according to the number of sections where it was simulated the fault. These considerations were taken in account in the cases 1 and 2.

### 5.2. Artificial intelligence-based master–slave strategy for the estimation of the fault section.

The implementation of master–slave strategy for the fault section estimation considers the dataset obtained in the Section 5.1 and the tuning hyperparameters presented in Table 5. In the slave stage, we obtain the ANN models that use the combination of features and hyperparameters proposed by the Cuckoo Search. The ANN model only can be obtained one time per location, i.e., if several chromosomes present the same gene with value of one, the same ANN model is used for these chromosomes.

## 6. Results and discussion

The results for the previous cases were analyzed according to the accuracy given by (7). The results are presented in the subsections below.

### 6.1. Case 1: ANN model as fault section estimator integrated into an IED

Fig. 10 shows the performance of the fault section estimator models for each IED installed along of the main grid and the MG, respectively. Here, we estimated the performance for each ANN model by using the default ANN parameters and using the Cuckoo Search-based tuning algorithm. When we observe the results, they show that the accuracy of the models varies according to the position of the IEDs not only for the grid but also for the MG. For instance, if we note the behavior of default parameters models, the ANN model with the best performance for the IEDs installed in main grid is IED 10 with an accuracy of 88.3%, whereas the model with the lowest performance is IED 1 with an accuracy of 80.8%. In this way, the IED location and the section size could be a factor that affect the performance of the ANN models. On the other hand, we can observe the ANN models with tuning and features selection which their performance shows an improvement between 2% and 6% for the models of IEDs installed in the main grid and an improvement between 1% and 5% in the models of IEDs installed in MG.

Complementary to Fig. 10, we can illustrate in Table 7 and 8 the best combination of features and tuning of hyperparameters that improved the performance of the ANN models for each IED. Hence, the IEDs that had the best performance for main grid and MG were 10 and 21, respectively, while the IEDs that presented the lowest performance were IED 1 and IED 19.

Table 9 and 10 present the confusion matrix for the IED 1 and IED 19. In Table 9 we can note that there is a improve in the IED1 which could be achieved by increasing the prediction in 4 and 8 (MG) sections with 12.2% and 11.8%, respectively. However, if we note the column associated to Section 8, we observe that the fault section estimator still presents a tendency to detect the faults into the MG (Section 8) instead of the main grid, especially in the prediction of faults in sections 4 and 6. On the contrary, Table 10 presents the confusion matrix for the IED 19 located into the MG. The results show that there is an increase in the performance of the IED19 model due to the improvement in the prediction of faults into the main grid (Section 4). However, the other section presents a reduction in their performance of faults prediction.

In general, the results obtained in this case present accuracies above of 86% for the IEDs of main grid and the MG. Despite of this, the models would work independently to select the fault section if there will be a failure of communication into the network., However, if the communication stills working, we can bring another option that will improve the performance of the fault section estimation.

### 6.2. Case 2 artificial intelligence-based master–slave strategy for the estimation of the fault section

The main grid protection system and the MG have 16 IEDs and 13 IEDs, respectively, which can be used by the centralized fault section estimation strategy. This strategy seeks to point out that there is an optimal number of IEDs that maximize the performance, we have varied the maximum number of IEDs that it can use both in the main grid and in the MG. Figs. 11 and 12 show the optimal number of IEDs that maximize the performance of the artificial intelligence-based master–slave strategy for the estimation of the fault section.

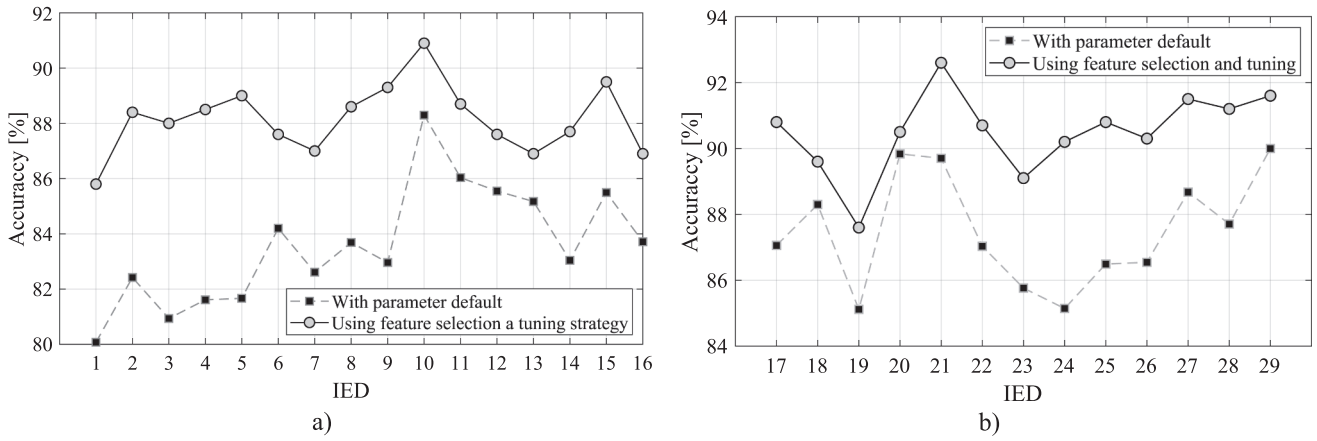


**Fig. 10.** Performance of ANN model a) IEDs located in the main grid; b) IEDs located in the MG.

**Table 7**
Best combination of features and tuning of hyperparameters for IEDs of the main grid.

| IED | Hyperparameters | Features | Accuracy [%] |
|---|---|---|---|
| 1 | 62,132,175,3, tanh, | 2,3,4,5,6,7,8,9,11,12,13,14,16,17,18 | 85.8 |
| 2 | 160,69,120,9, relu, | 2,3,4,5,6,7,8,9,10,12,13,15,16,17 | 88.4 |
| 3 | 117,197,107,2, relu, | 3,5,6,7,9,10,11,12,13,14,15,16,17,18 | 88.0 |
| 4 | 89,115,198,2, tanh, | 2,3,4,6,7,8,9,10,11,12,13,14,15,16,17,18 | 88.5 |
| 5 | 138,125,71,2, relu, | 1,2,3,4,5,6,7,8,9,10,11,12,13,14,15,16,17,18 | 89.0 |
| 6 | 35,44,66,9, tanh, | 3,4,5,7,8,9,11,13,14,15,16,18 | 87.6 |
| 7 | 146,73,86,1, relu, | 1,2,3,4,5,6,7,8,10,11,12,13,14,15,16,17 | 87.0 |
| 8 | 127,125,152,4, tanh, | 2,3,4,6,10,11,12,13,18 | 88.6 |
| 9 | 86,84,185,3, relu, | 2,3,4,5,7,8,10,12,13,16,18 | 89.3 |
| 10 | 112,105,158,7, relu, | 1,2,3,4,5,6,7,9,11,12,13,16 | 90.9 |
| 11 | 157,52,195,3, tanh, | 2,3,5,6,7,8,9,10,11,12,13,15,16,18 | 88.7 |
| 12 | 122,109,149,6, relu, | 3,4,5,7,8,9,10,11,12,13,14,15,16,17,18 | 87.6 |
| 13 | 128,151,143,8, relu | 2,3,4,7,9,10,15,17 | 86.9 |
| 14 | 101,164,93,6, relu, | 2,3,4,5,6,7,9,11,12,13,15,16,17,18 | 87.7 |
| 16 | 41,142,124,8, relu, | 1,2,3,4,6,8,9,13,14,15,16,17 | 86.9 |

**Table 8**
Best combination of features and tuning of hyperparameters for IEDs of the MG.

| IED | Hyperparameters | Features | Accuracy [%] |
|---|---|---|---|
| 17 | 192,172,148, relu, sgd, adaptive | 2,4,5,6,7,8,9,10,11,12,13,14,15,17 | 90.8 |
| 18 | 107,80,87,7, relu, sgd, adaptive | 2,4,5,6,8,9,11,12,13,15,16,17,18 | 89.6 |
| 19 | 130,168,148,7, relu, sgd, adaptive | 2,3,4,5,6,7,8,9,10,11,13,14,15,16 | 87.6 |
| 20 | 76,106,133,3, tanh, sgd, adaptive | 3,4,5,6,7,8,12,13,15,16,17,18 | 90.5 |
| 21 | 134,171,173,7, relu, sgd, adaptive | 4,5,7,8,9,10,11,13,14,15,16,17,18 | 92.6 |
| 22 | 177,112,72,6, tanh, sgd, adaptive | 1,2,4,5,6,7,8,10,11,13,15,18 | 90.7 |
| 23 | 121,180,134,1, tanh, sgd, adaptive | 2,4,5,6,7,8,10,11,13,14,15,16,17,18 | 89.1 |
| 24 | 111,114,52,4, tanh, sgd, adaptive | 2,3,4,5,7,8,9,12,13,14,15,16,17,18 | 90.2 |
| 25 | 144,140,170,5, relu, sgd, adaptive | 1,2,5,6,7,8,10,11,12,13,17 | 90.8 |
| 26 | 132,158,124,5, relu, sgd, adaptive | 2,4,5,6,7,8,9,10,11,12,13,14,15,17,18 | 90.3 |
| 27 | 83,138,131,8, tanh, sgd, adaptive | 1,2,4,5,6,9,10,14,15,16,18 | 91.5 |
| 28 | 170,179,146,3, tanh, sgd, adaptive | 1,4,7,8,9,10,11,12,13,14,15 | 91.2 |
| 29 | 97,91,146,3, tanh, sgd, adaptive | 2,3,4,5,7,8,9,10,11,12,13,14,15,16,17,18 | 91.6 |

Fig. 11 shows that for a maximum number of IEDs greater than 7 in the main grid, the number of IEDs selected by the proposed strategy tends to 7 and their performance is set at 95.5%. With the above, we can conclude that only 7 IEDs of 16 are necessary for the implementation of the proposed artificial intelligence-based master–slave strategy in the main network. A similar trend can be observed for the IEDs on the MG as shown in Fig. 12. Here, we can note the maximum number of IEDs is greater than 5, the number of IEDs selected by the proposed strategy tends to be 5 and its performance is established at 94.7%. This shows that only is necessary 5 IEDs of 13 for the MG to implement the proposed strategy.

On the other hand, we can illustrate the locations of IEDS selected by the strategy in Fig. 13 for the main grid and in the MG.

As a summary we can mention that the IEDs selected in the main grid were 2, 4, 6, 10, 12, 13, and 16, while the IEDs selected in the MG were 19, 21, 22, 24, 27, 28, and 29.

### 6.3. Comparison test

This section presents a comparison of the proposed FL strategy with three ML techniques, such as Support Vector Machine (SVM), Decision Tree (DT), and ANN. The comparison is made for the two cases analyzed in this research.

For case 1, ML models as estimators of the fault section are obtained using the Cuckoo Search-based tuning strategy. Table 11 compares the accuracy of the ML models obtained using DT and SVM for the IEDs with

**Table 9**
Confusion matrix for the IED 1 using default parameter and features selection and tuning strategy.

| CM | IED 1-ANN model with default parameter | | | | | | | | |
|---|---|---|---|---|---|---|---|---|---|
| | *1* | *2* | *3* | *4* | *5* | *6* | *7* | *8* | *0* |
| *1* | 375 | 2 | 0 | 0 | 0 | 0 | 0 | 9 | 0 |
| *2* | 2 | 165 | 0 | 2 | 3 | 0 | 0 | 1 | 0 |
| *3* | 0 | 0 | 463 | 10 | 0 | 5 | 0 | 14 | 0 |
| *4* | 0 | 3 | 47 | 631 | 1 | 99 | 4 | 121 | 0 |
| *5* | 0 | 1 | 0 | 0 | 130 | 4 | 0 | 0 | 0 |
| *6* | 0 | 1 | 3 | 49 | 5 | 207 | 0 | 164 | 0 |
| *7* | 0 | 0 | 1 | 0 | 0 | 0 | 105 | 3 | 0 |
| *8* | 0 | 0 | 0 | 86 | 1 | 98 | 0 | 706 | 0 |
| *0* | 0 | 0 | 0 | 0 | 0 | 0 | 0 | 0 | 188 |
| **CM** | **IED 1-ANN model with tuning and feature selection** | | | | | | | | |
| | *1* | *2* | *3* | *4* | *5* | *6* | *7* | *8* | *0* |
| *1* | 376 | 1 | 0 | 5 | 0 | 0 | 0 | 4 | 0 |
| *2* | 1 | 165 | 0 | 5 | 0 | 0 | 0 | 2 | 0 |
| *3* | 0 | 0 | 468 | 18 | 0 | 0 | 0 | 6 | 0 |
| *4* | 0 | 1 | 23 | 727 | 0 | 32 | 0 | 123 | 0 |
| *5* | 0 | 1 | 0 | 2 | 129 | 2 | 0 | 1 | 0 |
| *6* | 0 | 0 | 2 | 80 | 4 | 214 | 0 | 129 | 0 |
| *7* | 0 | 0 | 0 | 1 | 0 | 0 | 105 | 3 | 0 |
| *8* | 0 | 0 | 1 | 57 | 0 | 22 | 0 | 811 | 0 |
| *0* | 0 | 0 | 0 | 0 | 0 | 0 | 0 | 0 | 188 |

**Table 10**
Confusion matrix for the IED 19 using default parameter and features selection and tuning strategy.

| CM | IED 19- ANN model with default parameter | | | | |
|---|---|---|---|---|---|
| | *1* | *2* | *3* | *4* | *0* |
| *1* | 202 | 112 | 18 | 18 | 0 |
| *2* | 76 | 181 | 67 | 0 | 0 |
| *3* | 13 | 85 | 279 | 4 | 0 |
| *4* | 97 | 49 | 13 | 2135 | 0 |
| *0* | 0 | 0 | 0 | 0 | 360 |
| **CM** | **IED 19- ANN model with tuning and feature selection** | | | | |
| | *1* | *2* | *3* | *4* | *0* |
| *1* | 195 | 93 | 20 | 42 | 0 |
| *2* | 80 | 166 | 67 | 11 | 0 |
| *3* | 27 | 79 | 264 | 11 | 0 |
| *4* | 20 | 3 | 6 | 2265 | 0 |
| *0* | 0 | 0 | 0 | 0 | 360 |

higher and lower performance presented for the proposed strategy (PS).

The results show that the proposed strategy presents a higher precision in its ML models as estimators of the fault section when ANN is used. For the reference cases presented in Table 11, this improvement is up to 23% compared to the models obtained with DT and up to 10% compared to the models obtained with SVM.

For case 2, the artificial intelligence-based master–slave strategy is implemented using DT and SVM for the MG. Fig. 14 shows the optimal number of IEDs that maximize the performance the proposed strategy using DT, when the maximum number of IEDs is varied.

The results show a tendency of the strategy to maximize its performance when 4 IEDs are used, presenting an estimation accuracy of the faulted section of 87%. This shows that the proposed strategy increases its accuracy up to 10% when the communication system is available, and it can operate centralized way. However, it is also evident from the results that if the communication system is lost, each IED located in the MG will estimate the fault section with an accuracy higher than 79%. However, the performance of the strategy is still higher when ANN models are used.

On the other hands, Fig. 15 shows the optimal number of IEDs that maximize the performance the proposed strategy using SVM, when the maximum number of IEDs is increased.

The results show that the number of IEDs required by the centralized strategy to maximize its performance in locating faults in the MG is 4. With this number of IEDs, the strategy reaches a precision of 93.3%, being higher than the precision presented by the strategy using DT (87.2%), but lower than that presented by the strategy using ANN (95.5%). However, the number of IED necessary to maximize its performance is less than that presented by the previous strategies. This represents an advantage, since fewer ANN models would have to be integrated into the IEDs in the system.

## 7. Conclusions

This paper presented a master–slave strategy based on artificial intelligence for the fault section estimation for active distribution networks and microgrids using disperse measurements. Initially, this strategy was conceived in cases where there is a failure in a centralized communication. The strategy formulates a fault location scheme based on ANN models integrated to electronic intelligent device. The ANN model allows that each IED can obtain a fault section using only local current and voltage measures without a robust communication. Also, a feature selection and hyperparameter tuning strategy can be integrated and formulate to the strategy formulated to improve the performance of the ANN models. Additionally, the proposed strategy considered that, if a centralized communication system exists or is available, the fault section is determined by means of the individual estimations of the ANN models integrated to the IEDs of the system. As the accuracies of the IEDs are affected by their location in the system and it is not practical to consider ANN models for all the IEDs in the system. This paper

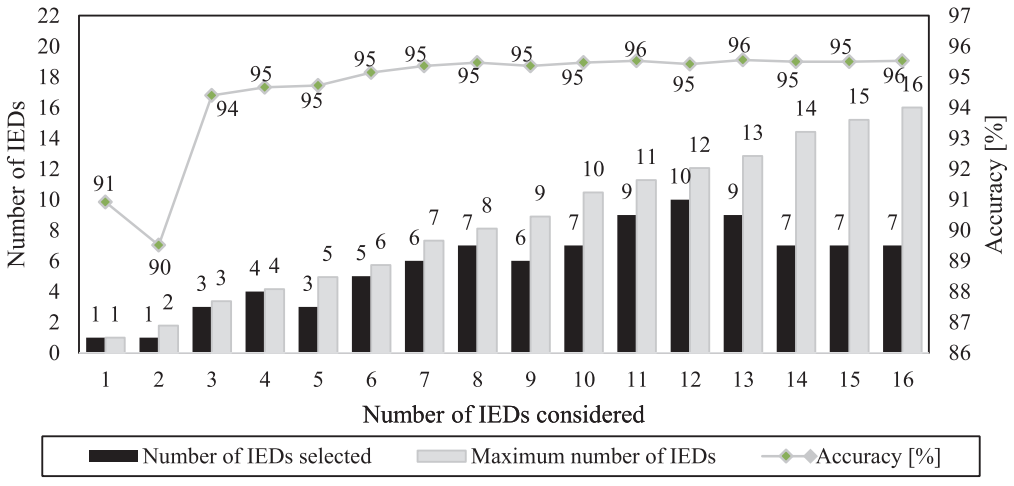


**Fig. 11.** Optimal location of IEDS for the main grid using the centralized master–slave strategy.

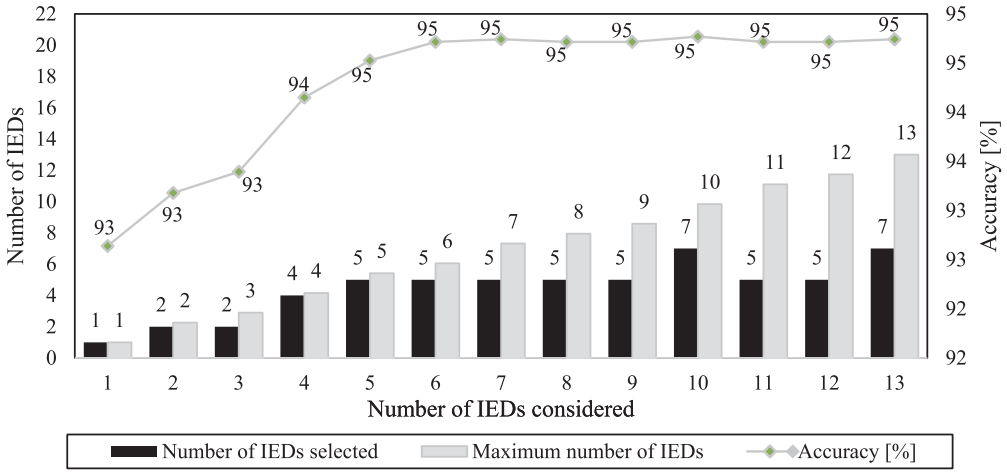


**Fig. 12.** Optimal location of IEDS for the MG using the centralized master–slave strategy.

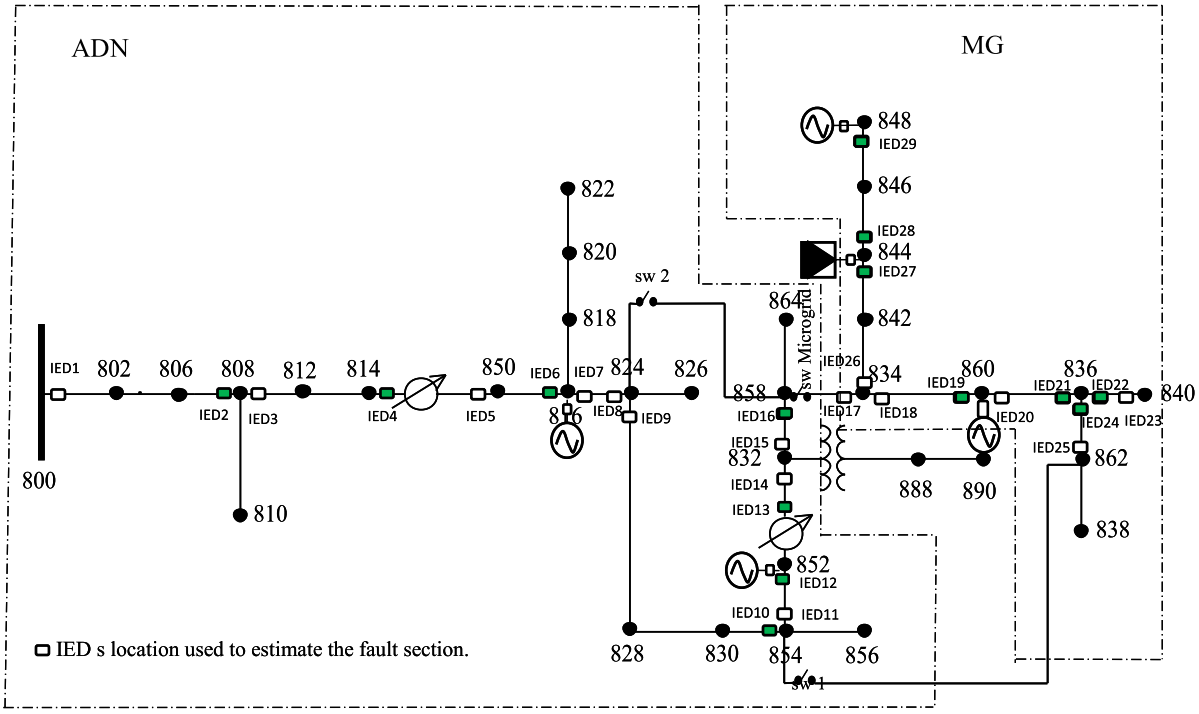


**Fig. 13.** Location of the IEDs into the network using the centralized master–slave strategy.

**Table 11**
Comparación de la estrategia de FL propuesta con tres técnicas ML.

| Grid | IED | Accuracy [%] | | |
|---|---|---|---|---|
| | | DT | SVM | PS |
| Main grid | 1 | 70,5% | 75,1% | 85,8% |
| | 10 | 67,1% | 83,4% | 90,9% |
| MG | 19 | 80,2% | 83,8% | 87,6% |
| | 29 | 79,2% | 88,0% | 92,6% |

formulates a master–slave strategy to determine the number of IEDs and their optimal location that maximizes the performance of the centralized fault section estimation strategy. The proposed strategy was validated in the modified IEEE 34-node test feeder. The results obtained show a performance higher than 80% of the ANN models obtained for IEDs when a centralized communication system is not used, nor is a hyperparameter tuning and feature selection strategy used. However, when the hyperparameter tuning and feature selection strategy is used, the performance of the ANN models obtained increases between 2% and 5%, presenting a performance greater than 86% for the ANN models. Finally, when the availability of the centralized communication system is considered, the master–slave strategy determined that the location performance of the fault section can be improved up to 95.5% using 7 IEDs placed a long of the main grid and at 94, 7% using 5 IEDs placed a long of the MG. The proposed strategy was compared with other machine learning models which show results above of 91%. The results presented above indicate a promising potential of the proposed strategy for real-life applications.

*CRediT authorship contribution statement*

**J. Atencia-De la Ossa:** Conceptualization, Methodology, Formal analysis, Investigation, Writing – original draft. **C. Orozco-Henao:** Conceptualization, Methodology, Formal analysis, Investigation,

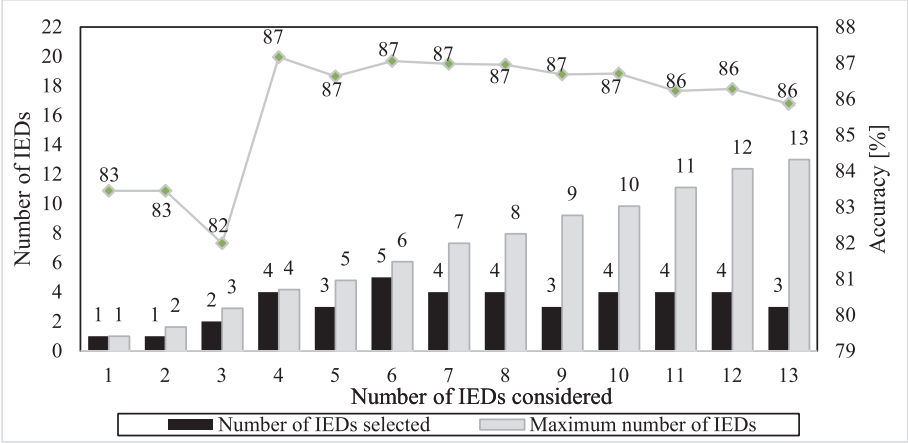


**Fig. 14.** Optimal location of IEDS for the MG using the centralized master–slave strategy and DT models.

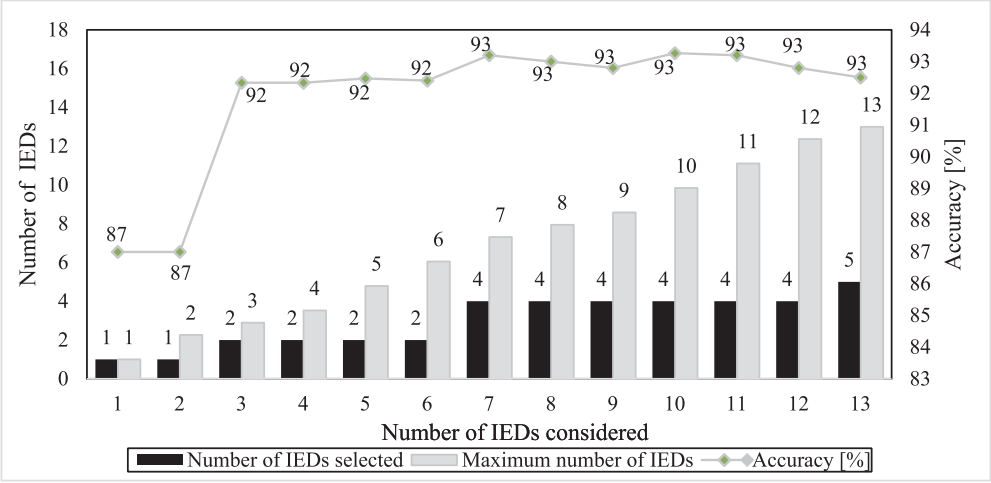


**Fig. 15.** Optimal location of IEDS for the MG using the centralized master–slave strategy and SVM models.

Writing – original draft. **J. Marín-Quintero:** Conceptualization, Methodology, Formal analysis, Investigation, Writing – original draft.

## Declaration of Competing Interest

The authors declare that they have no known competing financial interests or personal relationships that could have appeared to influence the work reported in this paper.

## Data availability

Data will be made available on request.

## Acknowledgments

This work was supported by Universidad del Norte, Fondo Nacional de Financiamiento para la Ciencia, la Tecnología e Innovación FCTEI del sistema general de regalías SGR, and Departamento Administrativo de Ciencia, Tecnología e Innovación - COLCIENCIAS (now Colombian Ministry of Science, Technology, and Innovation - Minciencias) by call contest "Convocatoria 809 de 2018: Formación de capital humano de alto nivel para las regiones - Atlántico '' and "Convocatoria 852 - Conectando conocimiento de 2019'' – Project Integra2023, code 111085271060, contract 80740-774-2020.

## References

[1] Ghadi MJ, Rajabi A, Ghavidel S, Azizivahed A, Li L, Zhang J. From active distribution systems to decentralized microgrids: a review on regulations and planning approaches based on operational factors. Appl Energy 2019:253. https://doi.org/10.1016/j.apenergy.2019.113543.

[2] Perez R, Vásquez C, Viloria A. A new approach to fault location in three-phase underground distribution system using combination of wavelet analysis with ANN and FLS. J Intell Fuzzy Syst 2019:1–11. https://doi.org/10.3233/jifs-18807.

[3] Bahmanyar A, Jamali S, Estebsari A, Bompard E. A comparison framework for distribution system outage and fault location methods. Electr Pow Syst Res 2017; 145:19–34. https://doi.org/10.1016/j.epsr.2016.12.018.

[4] Jamali S, Talavat V. Accurate fault location method in distribution networks containing distributed generations. Iran J Electr Comput Eng 2011;10:27–33.

[5] Orozco-Henao C, Bretas AS, Herrera-Orozco AR, Pulgarín-Rivera JD, Dhulipala S, Wang S. Towards active distribution networks fault location: contributions considering DER analytical models and local measurements. Int J Electr Power Energy Syst 2018:99. https://doi.org/10.1016/j.ijepes.2018.01.042.

[6] Orozco-Henao C, Bretas AS, Marín-Quintero J, Herrera-Orozco A, Pulgarín-Rivera JD, Velez JC. Adaptive impedance-based fault location algorithm for active distribution networks. Appl. Sci. (Switzerland) 2018:8. https://doi.org/10.3390/app8091563.

[7] Orozco-Henao C, Bretas AS, Leborgne RC, Herrera A, Martinez S. Fault location in distribution network with inverter-interfaced distributed energy resources in limiting current. In: Proceedings of International Conference on Harmonics and Quality of Power, ICHQP, vol. 2016- Decem; 2016. doi: 10.1109/ICHQP.2016.7783424.

[8] Bretas AS, Orozco-Henao C, Marín-Quintero J, Montoya OD, Gil-González W, Bretas NG. Microgrids physics model-based fault location formulation: analytic-based distributed energy resources effect compensation. Electr Pow Syst Res 2021: 195. https://doi.org/10.1016/j.epsr.2021.107178.

[9] Patcharoen T, Ngaopitakkul A. Fault classifications in distribution systems consisting of wind power as distributed generation using discrete wavelet

transforms. Sustainability (Switzerland) 2019:11. https://doi.org/10.3390/su11247209.
[10] Shi S, Zhu B, Lei A, Dong X. Fault location for radial distribution network via topology and reclosure-generating traveling waves. IEEE Trans Smart Grid 2019; 10:6404–13. https://doi.org/10.1109/TSG.2019.2904210.
[11] Xu Y, Zhao C, Xie S, Lu M. Novel fault location for high permeability active distribution networks based on improved VMD and S-transform. IEEE Access 2021; 9:17662–71. https://doi.org/10.1109/ACCESS.2021.3052349.
[12] Qiao J, Yin X, Wang Y, Xu W, Tan L. A multi-terminal traveling wave fault location method for active distribution network based on residual clustering. Int J Electr Power Energy Syst 2021:131. https://doi.org/10.1016/j.ijepes.2021.107070.
[13] Hosseinikia M, Talavat V. Comparison of impedance based and travelling waves based fault location methods for power distribution systems tested in a real 205-nodes distribution feeder. Trans Electr Electron Mater 2018;19:123–33. https://doi.org/10.1007/s42341-018-0004-1.
[14] Ledesma J, do Nascimento K, de Araujo L, Penido D. A two-level ANN-based method using synchronized measurements to locate high-impedance fault in distribution systems. Electric Power Syst. Res. 2020;188:106576. doi: 10.1016/J.EPSR.2020.106576.
[15] Perez R, Vásquez C, Viloria A. An intelligent strategy for faults location in distribution networks with distributed generation. J Intell Fuzzy Syst 2019;36: 1627–37. https://doi.org/10.3233/JIFS-18807.
[16] Tong Z, Lanxiang S, Jianchang L, Haibin Y, Xiaoming Z, Lin G, et al. Fault diagnosis and location method for active distribution network based on artificial neural network. Electr Power Compon Syst 2018;46:987–98. https://doi.org/10.1080/15325008.2018.1460884.
[17] Forouzesh A, Golsorkhi MS, Savaghebi M, Baharizadeh M. Support vector machine based fault location identification in microgrids using interharmonic injection. Energies (Basel) 2021:14. https://doi.org/10.3390/en14082317.
[18] Dashti R, Ghasemi M, Daisy M. Fault location in power distribution network with presence of distributed generation resources using impedance based method and applying Π line model. Energy 2018;159:344–60. https://doi.org/10.1016/j.energy.2018.06.111.
[19] Chaitanya BK, Yadav A. An intelligent fault detection and classification scheme for distribution lines integrated with distributed generators. Comput Electr Eng 2018; 69:28–40. https://doi.org/10.1016/j.compeleceng.2018.05.025.
[20] Kiaei I, Lotfifard S. Fault section identification in smart distribution systems using multi-source data based on fuzzy petri nets. IEEE Trans Smart Grid 2020;11:74–83. https://doi.org/10.1109/TSG.2019.2917506.
[21] Mirshekali H, Dashti R, Keshavarz A, Torabi AJ, Shaker HR. A novel fault location methodology for smart distribution networks. IEEE Trans Smart Grid 2021;12: 1277–88. https://doi.org/10.1109/TSG.2020.3031400.
[22] Bishop CM. Pattern recognition and machine learning (information science and statistics). Berlin, Heidelberg: Springer-Verlag; 2006.
[23] Pérez-Londoño S, Garcés A, Bueno-López M, Mora-Flórez J. Components modelling in AC microgrids. vol. 1. UTP editorial; 2020. doi: 10.22517/97895.
[24] Correa-Tapasco E, Mora-Flórez J, Perez-Londoño S. Performance analysis of a learning structured fault locator for distribution systems in the case of polluted inputs. Electr Pow Syst Res 2019;166:1–8. https://doi.org/10.1016/j.epsr.2018.09.016.
[25] Marín-Quintero J, Orozco-Henao C, Velez JC, Bretas AS. Micro grids decentralized hybrid data-driven cuckoo search based adaptive protection model. Int J Electr Power Energy Syst 2021;130:106960. https://doi.org/10.1016/j.ijepes.2021.106960.
[26] Eamonn K, Mueen A. Curse of dimensionality. In: Claude S, Webb GI, editors. Encyclopedia of machine learning and data mining. Boston, MA: Springer, US; 2017. p. 314–5. https://doi.org/10.1007/978-1-4899-7687-1_192.
[27] Panigrahi B k., Kiran A, Tripathy SK, Nanda RP. Location of fault on a microgrid using travelling wave and wavelet transform method. In: 2018 Second International Conference on Green Computing and Internet of Things (ICGCIoT) 2019. pp. 139–44. doi: 10.1109/icgciot.2018.8753038.
[28] Bengio Y. Practical recommendations for gradient-based training of deep architectures. Neural networks: tricks of the trade. Springer; 2013.
[29] Shahin MA, Holger MR, Jaksa MB. Data division for developing neural networks applied to geotechnical engineering. J Comput Civ Eng 2004;8:105–14. https://doi.org/10.1061/ASCE0887-3801200418:2105.
[30] el Aziz MA, Hassanien AE. Modified cuckoo search algorithm with rough sets for feature selection. Neural Comput Appl 2018;29:925–34. https://doi.org/10.1007/s00521-016-2473-7.
[31] Rodrigues D, Pereira L, Almeida T, Papa J, Souza A, Ramos C, et al. BCS: A Binary Cuckoo Search algorithm for feature selection. In: Proceedings - IEEE international symposium on circuits and systems; 2013. p. 465–8. doi: 10.1109/ISCAS.2013.6571881.
[32] Katoch S, Chauhan SS, Kumar V. A review on genetic algorithm: past, present, and future. Multimed Tools Appl 2021;80:8091–126. https://doi.org/10.1007/s11042-020-10139-6.
[33] Distribution System Analysis Subcommittee. IEEE 34 Node Test Feeder 2001.